

A NEW APPLICATION OF CFRP FABRICS IN EARTHQUAKE-RESISTANT RC BRIDGE PIERS

M. Saiidi¹, F. Gordaninejad², B. Gopalakrishnan³, and E. Reinhardt⁴

¹Department of Civil Engineering, University of Nevada, Reno, NV 89557; Email:
saiidi@unr.edu

²Department of Mechanical Engineering, University of Nevada, Reno, NV 89557

³California Department of Transportation, San Diego, CA 92121

⁴Department of Civil Engineering, University of Nevada, Reno, NV 89557

ABSTRACT

A new construction concept for structural frames consisting of concrete, steel, and carbon fiber composite fabrics was developed and implemented in a two-column bridge pier. Two new ideas are incorporated in the system. One is that the pier has pre-assigned column plastic hinges that are shifted away from column ends. Outside plastic hinges, the pier is to remain elastic. The other innovative concept incorporated in the frame is that where plastic hinging and ductility is required, steel reinforcement is used as the longitudinal reinforcement and where elastic behavior is required carbon fiber reinforced plastic (CFRP) sheets are used as the longitudinal reinforcement. FRP fabrics provide for confinement and shear capacity at all locations. A quarter-scale, two-column drop-cap pier with square columns was designed and constructed based on the aforementioned concepts. Normal strength concrete and Grade 60 mild steel were used in the frame. Unidirectional Replark carbon composite fabrics manufactured by the Mitsubishi Corporation were placed on the frame.

The frame was studied using computer programs DRAIN 3-DX and RC-Shake and a shake table testing program was developed. The shake table tests were completed in 2001. The frame was subjected to successive runs of the 1994 Northridge-Sylmar record with increasing amplitudes until failure. The plastic hinges behaved as planned, and the failure occurred after the rupture of the FRP fabrics in one of the plastic hinges. The strain data confirmed the location of plastic hinges and the relatively small strains in areas that were intended to remain elastic. Minor cracking of the beam-column joints revealed after the removal of the CFRP fabrics indicated a need for slight refinement of the CFRP design in the joint regions.

INTRODUCTION

A large number of bridges in the United States are considered to be deficient. A substantial number of them suffer from deterioration due to environmental effects. The high cost of

maintenance and repair in addition to issues related to public safety and disruption of traffic during repair work has necessitated an examination of nontraditional materials for possible adaptation in bridge engineering. One of the promising solutions for durable and reliable designs of future bridges can be the use of FRPs with superior characteristics instead of conventional civil engineering materials. Therefore, the development and application of advanced composite materials for design, repair, and retrofit of bridges are key issues that are being considered by researchers. To date, the application of FRPs in structural design of new construction (as opposed to retrofit application) has been relatively scarce. Glass and carbon fiber reinforced plastic sections and bars have been used for specialized applications (Ballinger (1991), Mirmiran et al. (1999)). Their use in new structural systems has been limited primarily due to the lack of sufficient research data and standards.

An innovative concept was explored in the present study, wherein steel reinforcement was used to provide ductility capacity and to control the failure mode, and CFRP fabrics were used to provide shear reinforcement, confinement and longitudinal reinforcement where elastic behavior is needed. In addition, the hinge zones were relocated (Abdel-Fattah and Wight (1987), Galunic and Bertero (1977)) away from member ends to ensure that damage can be limited and controlled within plastic hinge zones which are specially detailed, while all other portions of the structure remain essentially elastic at all times. The primary goal of the study was to determine if a conventional civil engineering material, such as reinforced concrete, would work with an advanced composite material like carbon fibers, to provide an alternative to bridge substructure construction.

TEST STRUCTURE

A two-column pier was constructed, reinforced with steel reinforcement and carbon fiber reinforced plastic (CFRP) laminates, and tested to failure on a shake table. The pier was constructed to $\frac{1}{4}$ scale so that it could be accommodated on a 20 ft. x 20 ft. (6.1m x 6.1m) shake table. Figure 1 shows the bent dimensions and the composite layout. The lines within the elements show the direction of carbon fibers. Figure 2 shows beam and column cross-sections. Plastic hinges in the columns were offset by terminating the #5 bars some distance away from the column ends as shown in Fig. 2. The bent dimensions were chosen to reflect those of typical highway two-column bents. The entire beam length and column middle regions were designed to remain elastic. Hence, composites were used for longitudinal reinforcement in these locations. Minimal longitudinal steel bars were provided for reinforcement of the beams and columns, also #4 stirrups were used at 9 in. spacing to reinforce the frame before the composites were installed and to resist loads induced in the frame during its transportation. Two horizontal and two vertical layers of CFRP fabrics were provided at each joint on both sides of the bent for joint shear reinforcement. The joint shear design was based on the ACI 352 provisions (2000).

The concrete used in the pier was normal-weight concrete with a maximum aggregate size of 10 mm (3/8 in.). Portland cement type I was used. The target concrete compressive strength was 5 ksi (34 MPa), while the actual strengths were 6.26 ksi (42.8 MPa) in the columns and 5.29 ksi (36.1 MPa) in the beam on the day of testing. The concrete was air cured, and subsequently the surface of the concrete was prepared for laminate application. The steel bars were of Grade 60

with a measured yield stress of 63.5 ksi (438 MPa). The Mitsubishi CFRP product, Replark Type 30, was used. First the surface was ground using a disk grinder, then putty (supplied by the manufacturer of the composites) was applied to smooth out rough spots. Next, a layer of resin undercoat was applied followed by a layer of carbon fiber sheet. This process was repeated for all the layers. The composite installation was completed by application of a resin overcoat. Any air bubbles trapped beneath the laminate were repaired by injecting epoxy into the voids.

The specified lamina elastic modulus in the fiber direction was 33,400 ksi (228 GPa) while its tensile strength along the fiber direction was 493 ksi (3.365 GPa). Coupons were also tested by the researchers, and the lamina elastic modulus in the fiber direction was found to be 38,400 ksi (262.3 GPa) while its tensile strength along the fiber direction was 379.8 ksi (2.593 GPa). The measured lamina elastic modulus perpendicular to the fiber direction was 509.6 ksi (3.48 GPa) and its tensile strength perpendicular to the fiber direction was 1.76 ksi (12 MPa).

EXPERIMENTAL PROGRAM

The test setup is shown in Fig. 3. The footings were fixed to a 20 ft x 20 ft (6.1 m x 6.1 m) shake table using threaded bars. The bent was extensively instrumented with strain gages, displacement transducers (to measure displacements and curvatures), accelerometers and a load cell (to measure lateral load applied to the specimen). For simulating a vertical load of 6.1 kip/ft (88.6 kN/m) on the beam, ten threaded bars running between the loading frame and the transfer beam were stressed to 6.4 Kip (28.5 kN) each using hydraulic rams. The beam was rigidly attached to the shake table through steel brackets (Fig. 3). The brackets served a dual purpose – that of restraining the pier from horizontal slippage and also anchoring the threaded rods. A system of accumulators was attached to the rams to minimize axial load fluctuation. To replicate the inertial effect of the gravity loads, a mass rig was used, which consisted of a pinned steel frame mechanism supporting concrete reaction blocks. The mass rig had an effective lateral inertial load of 64 kips and it was connected to the loading frame by a pinned-pinned steel tube.

The earthquake record used to drive the shake table was the January 17, 1994 Northridge earthquake as measured at the Sylmar Hospital. This record was chosen due to its being representative of a typical near-fault earthquake in the western United States. Furthermore, analytical studies showed that this record would lead to high ductility demand thus allowing for ultimate behavior testing. Since the test specimen was a scaled model of the prototype column, the earthquake record time axis was scaled by a factor of 0.5 to create a response in the test specimen that would parallel the prototype column. The testing was completed by applying scaled versions of the strong motion accelerogram. The test consisted of thirteen events beginning with pre-yield loading and continuing until visible column failure occurred.

ANALYTICAL MODELING

The computer analysis of the specimen was completed using two special-purpose programs for nonlinear dynamic structural analysis (DRAIN 3DX and RC-Shake). The moment-curvature relationships were calculated using RCMC (Wehbe et al. 1997). RC-Shake is a computer

program that calculates the dynamic response of a structure modeled as a single-degree-of-freedom (SDOF) nonlinear system, considering both hysteretic and viscous damping, as well as the loading setup of the mass rig system. A degrading stiffness hysteresis model, called the Q-hyst, models the nonlinear load-deformation response (Saiidi, 1982). The input to the program requires a bi-linear load-displacement relationship. The output of the program includes the force-displacement response of the SDOF system. The structure was also modeled using DRAIN 3DX software, which was used for push-over analysis to obtain the static load-displacement relationship of the specimen in addition to internal moments, shears, etc.

TEST RESULTS

The target peak table acceleration for the first event was 0.06g which is 10 percent of the peak acceleration in the original Sylmar record. At this amplitude the column force was well below the yield force. At a peak acceleration of 0.18g, cracks were seen in the transverse layer of composites at the bottom of the columns. At 1.05g, a crack in the concrete at the joint between the right column and beam was noted. After this run the final run with a peak acceleration of 1.2g was applied. During this run, a part of the confinement composite layer failed near the bottom of the right column in the plastic hinge region. Also, the confinement composite layer at the top of the right column delaminated from the column. The measured displacement ductility during the final run was approximately 6.

Load-Displacement Response

The force-displacement hysteresis curve for all the runs is plotted in Fig. 4. The first few events resulted in mostly linear loops, however at larger peak table accelerations, the loops were non-linear. Large energy dissipation is seen in Fig. 4, indicating that considerable inelastic deformations took place at the plastic hinges as planned.

The measured and calculated force-displacement envelopes at the top of the pier are shown in Fig.5. Figure 5 also shows the peak forces achieved at different peak table accelerations. It is seen that stiffness reduced progressively with increasing acceleration, indicating progressive yielding at the hinges. The change in stiffness at 0.18g, 0.75g and 0.90g is noteworthy. Figure 5 also shows the measured force-deflection plot obtained using the DRAIN 3D computer model prior to the tests using specified material properties. It can be seen that the measured initial stiffness was in excellent agreement with the calculated stiffness, with differences being less than 1 percent. At larger lateral loads, the measured stiffness was lower than calculated values. This may be because p-delta effects were not accounted for in the analytical model.

Steel Bar Strains

Peak strains in the column plastic hinge steel bars were close to 20,000 microstrains at 8" (200 mm) below the bottom of beam and 8" (200 mm) above top of footings. The peak strains on hinge bars closer to the beam were less than these values indicating that the hinges were successfully offset by 8" (200 mm) as intended. Figure 6 shows the combined measured strain hysteresis data for all the run at the lower plastic hinge in the left column. The measured peak

strain was approximately nine times the measured yield strain of the bars, which was 2190 microstrains. The bar yielded during the run with peak amplitude of 0.4xSylmar. It reached the peak strain of 19,690 microstrains during 1.9xSylmar and peak strain of 17,650 during 2xSylmar.

Peak strains in beam bars at the face of the columns were less than 3,000 microstrains. The level of strain in the top and bottom bars was comparable. Figure 7 shows the strain hysteresis curves for the bottom beam bar at the face of the right column. Yielding in the beam bars did not initiate until 1.5xSylmar. The peak strains in the beam bar shown in Fig. 7 were 2910 and 2820 microstrains during 1.9 and 2xSylmar motions, respectively. Note that the beams were intended to remain elastic. However, the maximum beam bar strain during the earthquakes reached 1.3 times the yield strain and exceeded the target level.

CFRP Jacket Strains

Peak strains in gages on the transverse composite layers on the columns at the hinge regions were about 4,000 microstrains, less than the assumed design strain of 10,800 microstrains. The strain hysteresis curves for transverse fibers in the lower plastic hinge of the left column are shown in Fig. 8. The force-strain relationship was nearly linear until the 1.9xSylmar motion was applied. At the end of this run a permanent strain of 1170 microstrains was observed. As mentioned in previous sections, the jacket on the lower plastic hinge in the right column failed during 2xSylmar. No strain gages were installed at the location of jacket failure, and, hence, the maximum strain could not be determined.

The tensile strains in composite fabrics parallel to the column were less than 2,000 microstrains, well below the failure strain of 14,000 microstrains. Strain in composite layers on the beam parallel to the beam axis were less than 3,000 microstrains, implying that the beam composite fabrics did not suffer any damage, as planned. Also, strains in the beam composite fabrics perpendicular to the beam, which were used for shear reinforcement, were less than 1,500 microstrains, meaning that the beam shear design was adequate.

The maximum strains in the composites in the joint region were below 1,500 microstrains. Figure 9 shows the force-strain relationship for CFRP jacket at mid-depth of the right joint region measured with a horizontal strain gage. It can be seen that the strain was always tensile regardless of the direction of motion because there was always a tendency for the joint to form a diagonal tension crack extending from the upper left to the lower right under pull forces and upper right to the lower left under push forces. Even though the peak strain in the joint jacket was small, upon removal of the composite layer after the final shake table test, cracks were seen in the joint indicating that the joint design procedure may need to be reviewed.

The composite layers were removed after the test, in order to survey the damage locations and evaluate crack patterns. The composite layers had delaminated near the hinge regions and at the joints, hence removal was possible. Horizontal cracks were noted at the hinge region, which was to be expected because no vertical composite fibers were present in this area. However, a number of shear cracks at about 45° were noted in the hinges in the right column. These cracks are believed to have formed after the confinement CFRP was ruptured (see Fig. 10). Shear

cracks in the joint region were also noticed, as shown in Fig. 10, which may mean that additional CFRP layers may be necessary. The composite layers in the beam and the part of the columns in between plastic hinges did not delaminate, meaning that these regions remained elastic as was intended.

CONCLUSIONS

The exploratory study presented in this article demonstrated the feasibility of using CFRP fabrics in combination with concrete for eventual application in new highway bridge piers. The new design is particularly attractive in bridges where durability is of concern, and where steel reinforcement congestion is a problem. The pattern of damage observed after removal of the CFRP jackets showed that the design was generally successful. The strains were relatively high in the preassigned plastic hinges and relatively low elsewhere. Failure occurred in the transverse composite jacket in one of the preassigned plastic hinges.

The study showed that, to completely eliminate damage in the joint region and to keep the beam bars strains in the elastic range, the number of CFRP fabric layers in the joint and the beam would have to be increased.

The preliminary comparison of the analytical and experimental results indicated that familiar constitutive relationships used for concrete and steel may be used to estimate the strength of concrete-carbon fiber laminate sections.

ACKNOWLEDGEMENTS

The study presented in this article was funded by the US National Science Foundation (NSF) Grant CMS 980080. The authors are thankful to NSF and Dr. Jack Scalzi, the NSF program director, for the support. The authors are also indebted to Dr. Ali Ganjehlou of Mitsubishi for donating the Replark material and for providing guidance in installation of the fabrics.

REFERENCES

- Abdel-Fattah, B. and Wight, J. K. (1987). Study of Moving Beam Plastic Hinging Zones for Earthquake-Resistant Design of R/C Buildings. *ACI Structural Journal* **84:S4**, 31-39.
- ACI-ASCE Committee 352, (2000). *Recommendations For Design of Beam-Column Connections in Monolithic Reinforced Concrete Structures*, ACI. Detroit, USA.
- ACI Committee 318 (1995). *Building Code Requirements for Structural Concrete*, American Concrete Institute (ACI), Detroit, USA.
- Ballinger, C. A. (1991). Development of Composites for Civil Engineering. *Proc., the First Advanced Composite Mat. in Civ. Engrg. Struct. Conf.*, ASCE, New York, N. Y., 288-300.

Galunic, B., Bertero, V. V., Popov, E. P. (1977). *An Approach for Improving Seismic Behavior of Reinforced Concrete Interior Joints*, Report No. UCB/EERC-77/30, University of California, Berkeley.

Kono, S., Inazumi, M. and Kaku, T. (1998). Evaluation of Confining Effects of CFRP Sheets on Reinforced Concrete Members. *Proc. Second Int. Conf. on Composites in Infrastructure*, Department of Civil Engr and Engr Mech, Univ of Arizona, Tucson, Arizona, 343-355.

Mander, J. B., Priestley, M. J. N., and Park, R. (1988). Theoretical Stress-Strain Model for Confined Concrete Columns. *ASCE Journal of Structural Engineering* **114:8**, 1804-1826.

Mirmiran, A., Shahawy, M., Samaan, M. (1999). Strength and Ductility of Hybrid FRP-Concrete Beam-Columns, *ASCE J. Struct. Eng.* **25:10**, 1085-1093.

Saiidi, M. (1982). Hysteresis Models for Reinforced Concrete, *Journal of Structural Division, Proc of the ASCE*, **108:5**, 1077-1087.

Wehbe, N., Saiidi, M. and Gordaninejad, F. (1994). Behavior of Graphite/Epoxy Concrete Composite Beams. *ASCE Journal of Structural Engineering* **120:10**, 2958-2976.

Wehbe, N. I., Saiidi, M. S., and Sanders, D. H. (1997). *Effects of Confinement and Flares on the Seismic Performance of Reinforced Concrete Bridge Columns*, Report No. 97-2, CCEER. Department of Civil Engineering, University of Nevada, Reno, September 1997.

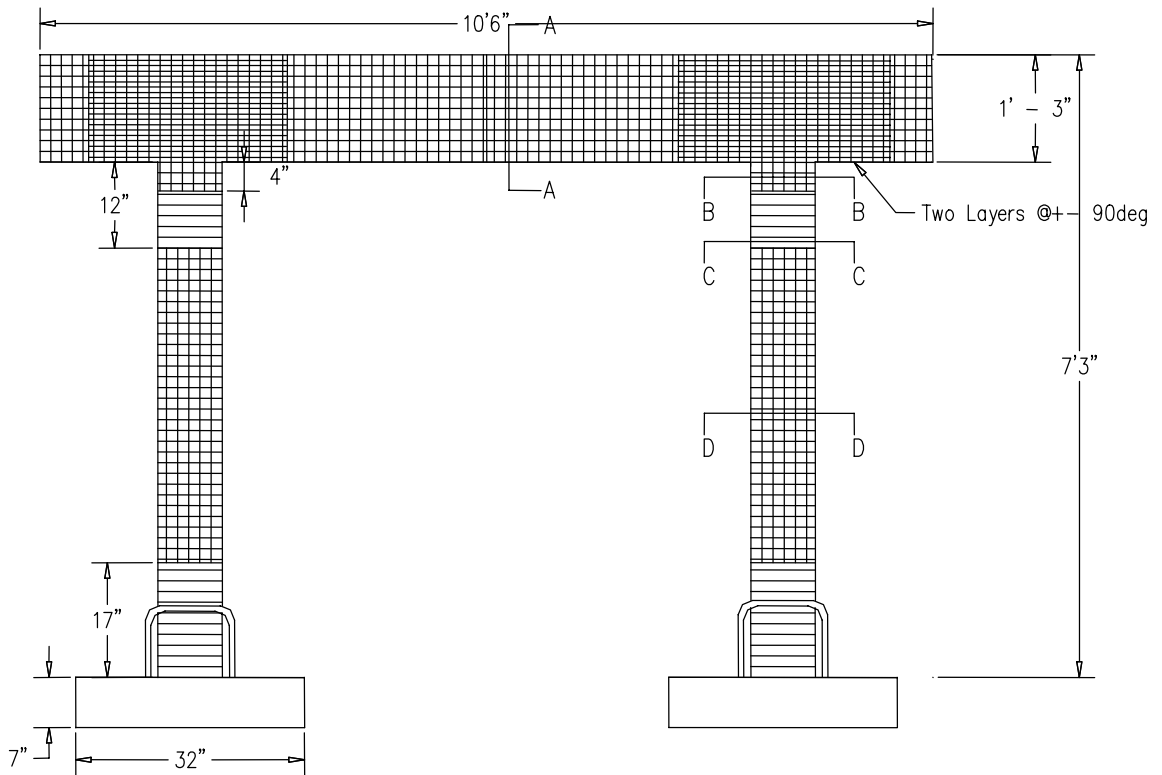


Figure 1: Dimensions of pier and arrangement of composites

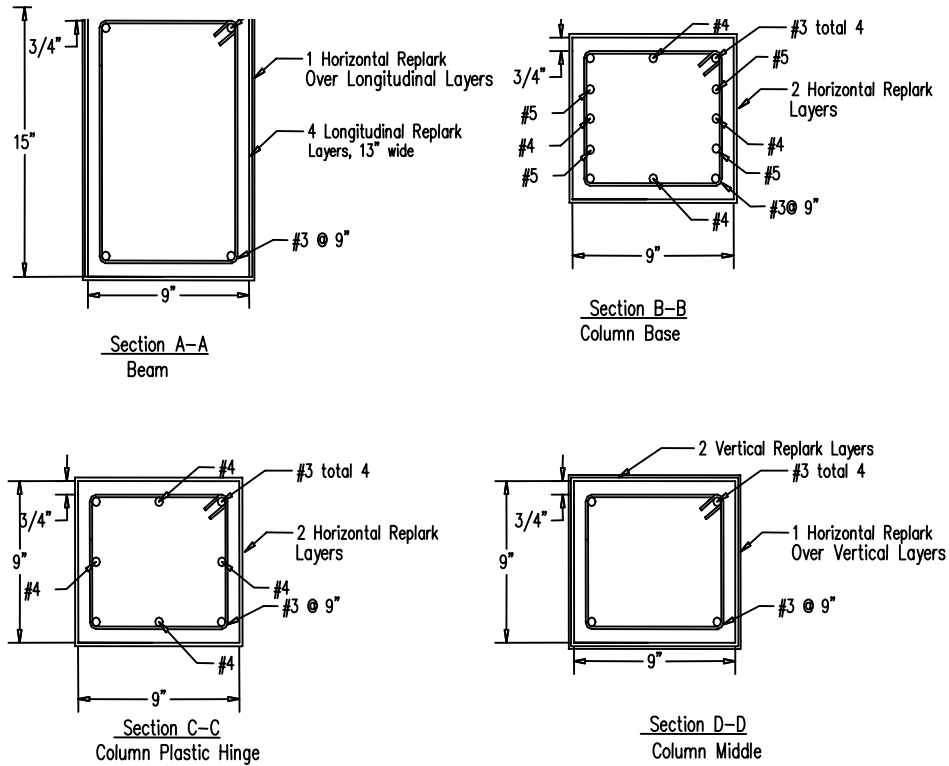


Figure 2: Pier section details and composite layout

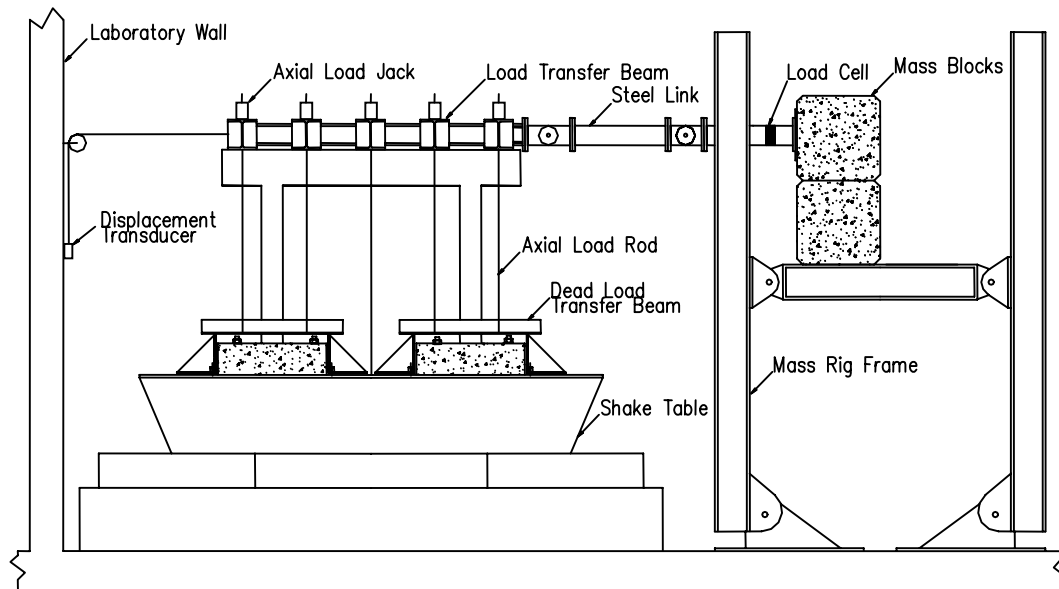


Figure 3: Shake table test setup

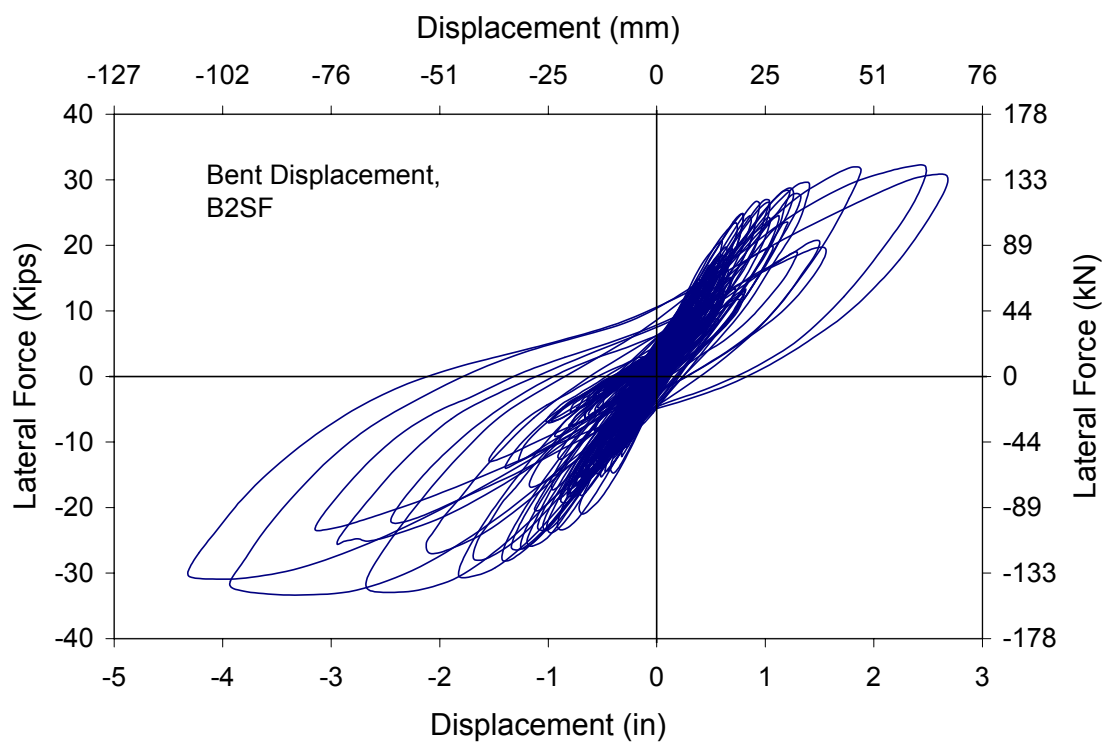


Figure 4: Force-displacement hysteresis relationship

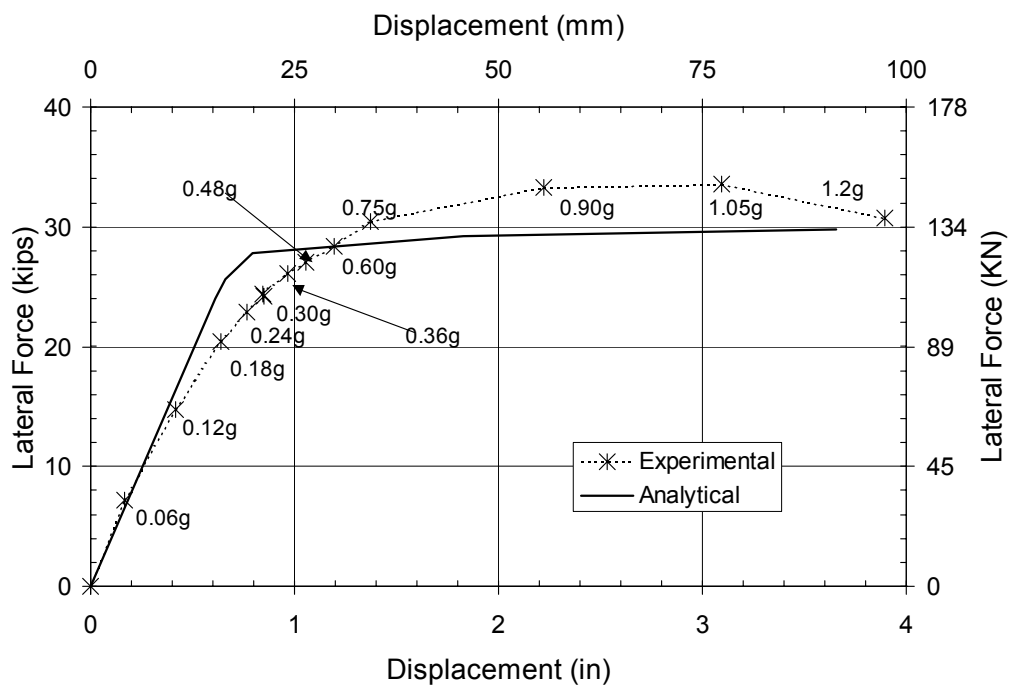


Figure 5: Force-displacement envelopes

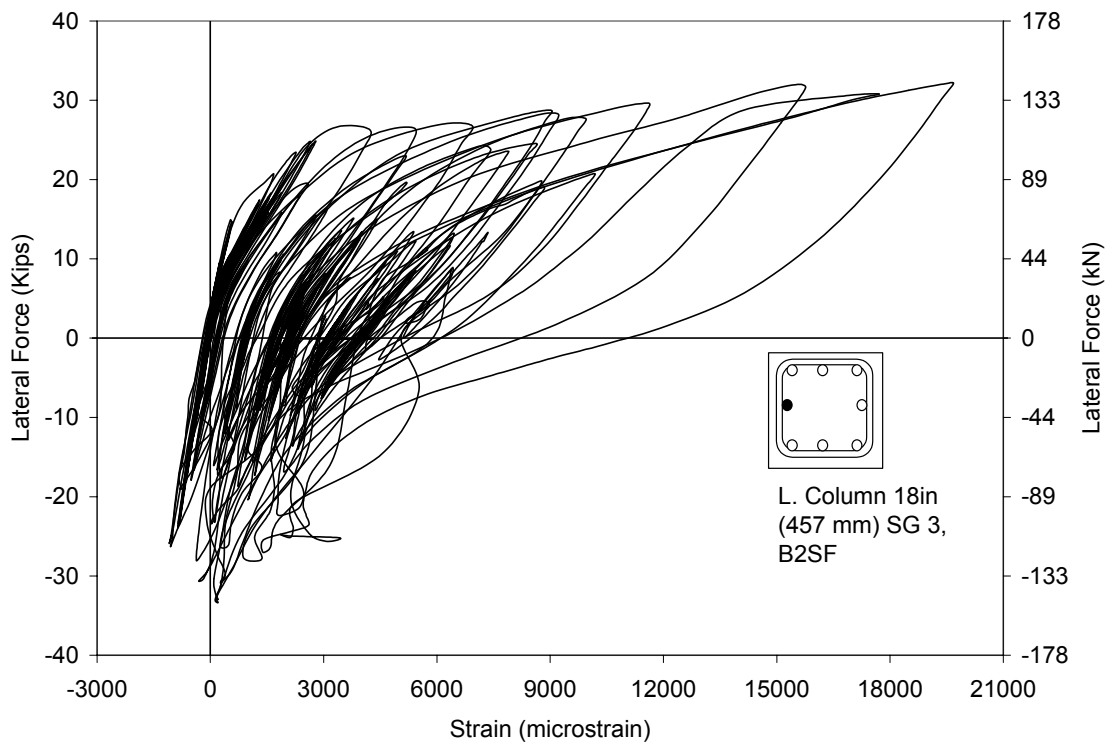


Figure 6: Column bar hysteresis relationship

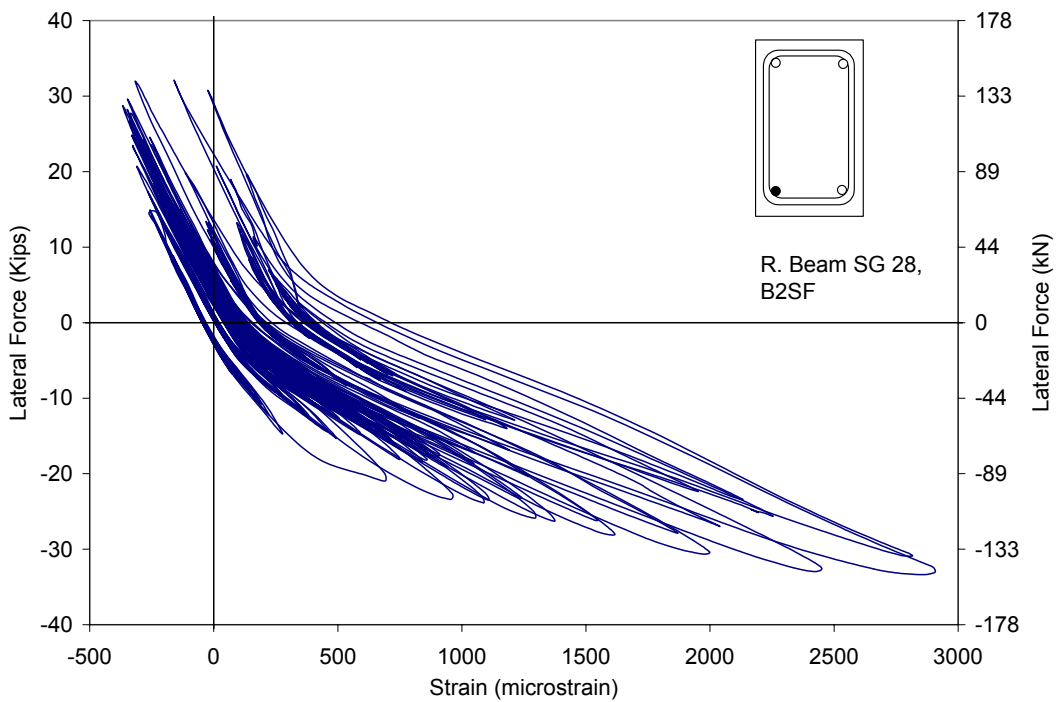


Figure 7: Beam bar hysteresis relationship

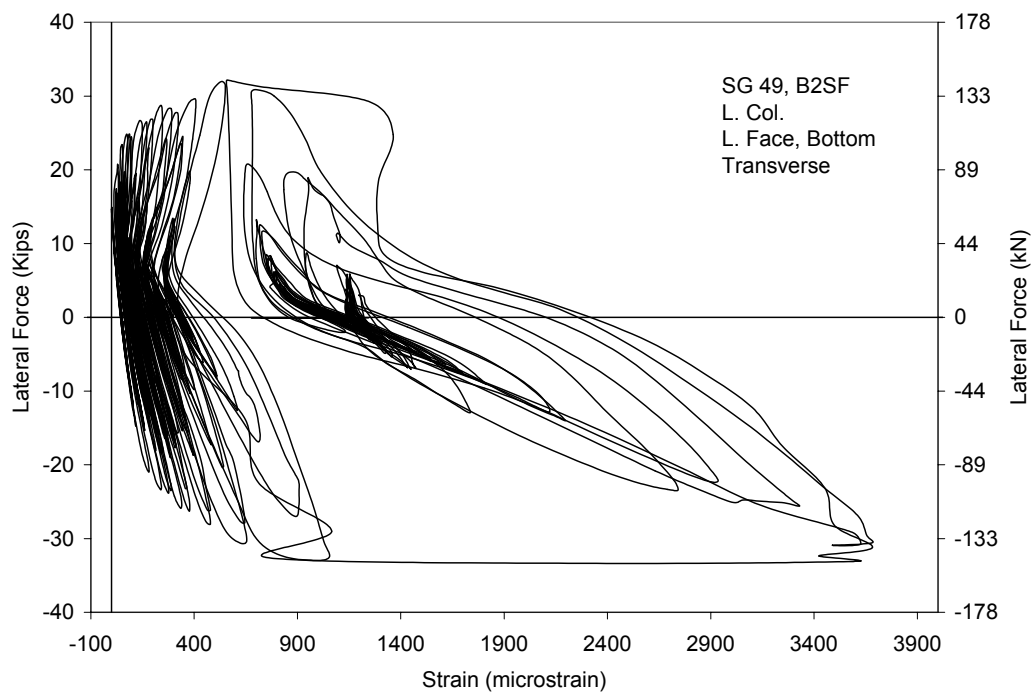


Figure 8: Transverse CFRP hysteresis relationship

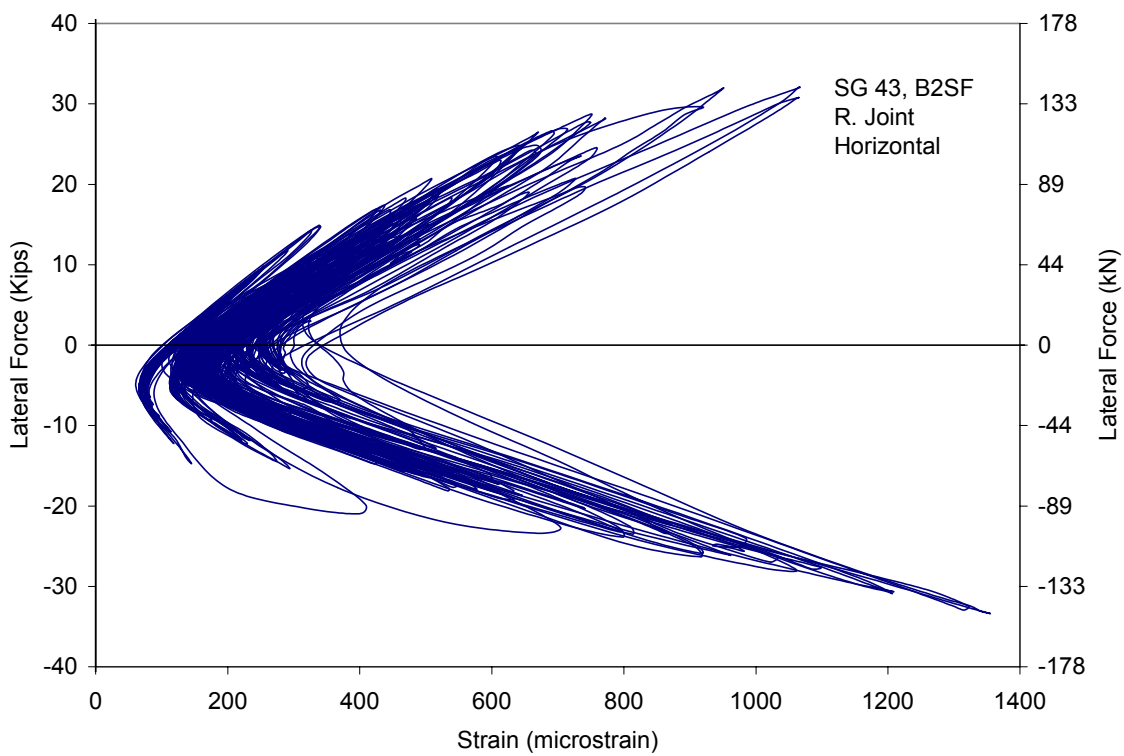


Figure 9: Joint CFRP hysteresis relationship

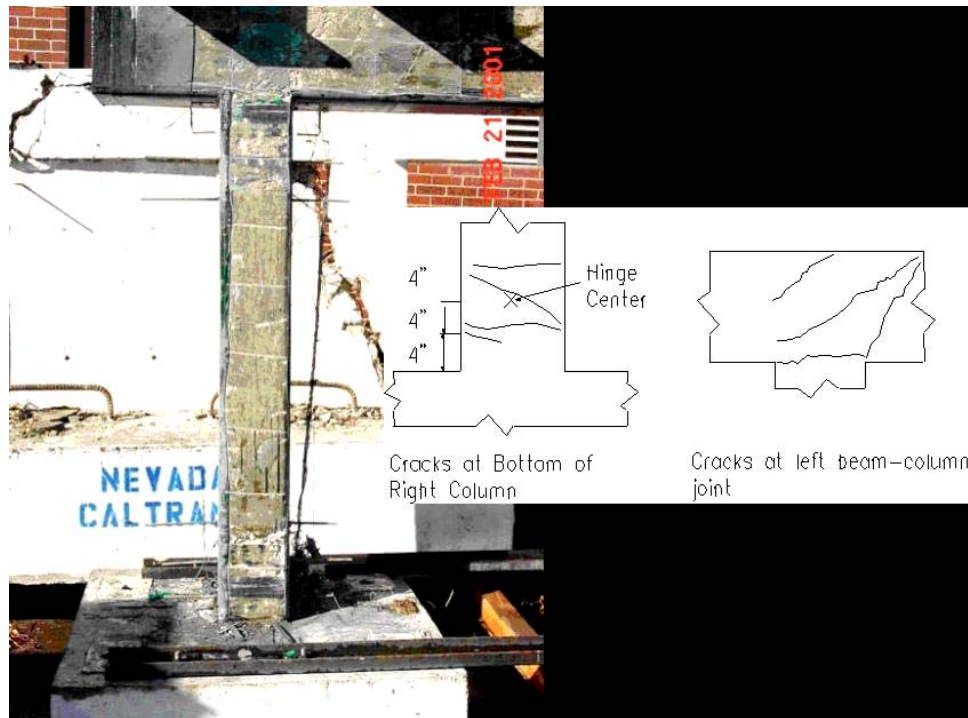


Figure 10: Post-failure crack patterns